



Room 14-0551
77 Massachusetts Avenue
Cambridge, MA 02139
Ph: 617.253.5668 Fax: 617.253.1690
Email: docs@mit.edu
<http://libraries.mit.edu/docs>

DISCLAIMER OF QUALITY

Due to the condition of the original material, there are unavoidable flaws in this reproduction. We have made every effort possible to provide you with the best copy available. If you are dissatisfied with this product and find it unusable, please contact Document Services as soon as possible.

Thank you.

Some pages in the original document contain color pictures or graphics that will not scan or reproduce well.

A New Surgical Model for Studying the Healing Response of Renal Tissue in the Presence of Collagen-Glycosaminoglycan Matrices

by

Roy Kuniaki Esaki

Submitted to the Department in Partial Fulfillment of the Requirements for the Degree of

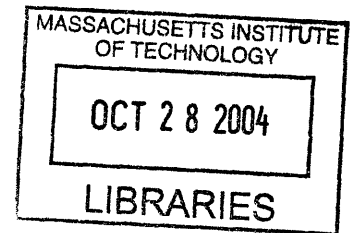
Bachelor of Science

at the

Massachusetts Institute of Technology

June 2004

© 2004 Roy Esaki
All Rights Reserved



The author hereby grants M.I.T. permission to reproduce and distribute publicly paper and electronic copies of this thesis in whole or part

Signature of Author *[Handwritten Signature]*
Department of Mechanical Engineering, MIT
May 7, 2004

Certified by *[Handwritten Signature]*
Ioannis V. Yannas
Professor of Mechanical Engineering
Thesis Supervisor

Accepted by *[Handwritten Signature]*
Ernest G. Cravalho
Department of Mechanical Engineering
Chairman, Undergraduate Thesis Committee

A New Surgical Model for Studying the Healing Response of Renal Tissue in the Presence of Collagen-Glycosaminoglycan Matrices

By Roy K. Esaki

Submitted to the Department of Mechanical Engineering on May 7, 2004 in Partial Fulfillment of the Requirements for the Degree of Bachelor of Science in Mechanical Engineering

ABSTRACT

The treatment of renal trauma can involve the surgical removal of part of a patient's kidney, which leads to scarring, distortion of the renal architecture, and potentially renal insufficiency. Current research suggests that the implantation of collagen-glycosaminoglycan (GAG) extra-cellular matrices after traumatic renal injury prevents contraction, decreases scarring, and may ultimately induce the regeneration of functional renal tissues after injury. The goal of the current study was to develop a new surgical model to study the effects of the matrices on the healing of traumatic renal wounds.

Four hemispherical, reproducible wounds were created in the cortex of the left kidney of 20 adult male rats (*Rattus norvegicus*). Three wounds were each filled with one of three types of matrices, while the fourth remained empty to serve as a control. Four weeks post-operatively, the animals were sacrificed and kidneys were processed by standard histological methods.

All animals tolerated the procedure well, and 16 kidneys were included in the final analysis. After four weeks of healing, contraction had occurred in all of the wounds, and a lacuna, a crater-like depression with a raised lip around the perimeter, had formed around the wound site. One of the matrices, with an average pore diameter of 182 μm , decreased the lacuna area by 37% ($p=0.006$) and the wound area by 26% ($p=0.003$), but did not significantly affect collagen deposition. One of the other matrices, with an average pore diameter of 101 μm , significantly reduced the lacuna area by 43% ($p=0.005$) and the wound area by 41% ($p=0.009$) as compared to the untreated control. This matrix also decreased the extent of collagen deposition by 42% ($p=0.04$); this represents a reduction in the formation of fibrotic tissue, which is a highly desirable objective with respect to the goal of achieving regeneration of functional tissue.

These results demonstrate that such collagen-GAG matrices affect wound contraction, and possibly tissue regeneration, although the exact mechanisms could not be determined in this study. A finite element analysis, modeling the geometry of wound closure using data from the alpha-smooth muscle actin stains, should be conducted in a future study to elucidate the healing mechanism, and to allow the present data regarding the effect of the matrix on wound geometry to be better interpreted.

Thesis Supervisor: *Ioannis V. Yannas,*

Title: *Professor of Mechanical Engineering and Professor of Biological Engineering*

TABLE OF CONTENTS

ABSTRACT.....	2
TABLE OF CONTENTS.....	3
ACKNOWLEDGEMENTS:	5
CHAPTER 1 – INTRODUCTION.....	6
1.1 – Renal Trauma.....	6
1.2 – In Vivo Tissue Regeneration: Prior Art.....	7
1.3 – Renal Tissue Engineering: Background and Prior Art	7
1.4 – Goals of the Current Study	8
CHAPTER 2 – MATERIALS AND METHODS	11
2.1 – Matrix Fabrication	11
2.2 – Experimental Paradigm.....	13
2.3 – Implantation Surgery Protocol.....	14
2.4.– Post-operative care.....	20
2.5 – Animal Sacrifice and Kidney Removal Surgery.....	20
2.6 – Morphology.....	21
2.6.1 Gross Morphology	21
2.6.2 Histology and Immunohistology.....	22
2.6.3 Image Analysis of Histological Slides.....	22
2.6.3 Statistical Methods.....	23
CHAPTER 3 – RESULTS.....	24
3.1 – Surgical and Post-Operative Outcomes	24
3.2 – Reproducibility of Surgical Protocol	24
3.3 – Geometry of Healing.....	25
3.3.1 Description of Wound Site.....	25
3.3.2 Wound Area.....	26
3.3.3 Lacuna Area.....	28
3.4 – Tissue Morphometric Data (Histological Data).....	29
3.4.1 Abnormal Tissue Area	29
3.4.2 Collagen Deposition.....	30
CHAPTER 4 – DISCUSSION.....	33
4.1 – Summary of Matrix Effects	33
4.2 – Paired versus Unpaired Statistical Analysis	33
4.3 – Reproducibility of Surgical Protocol	34
4.4 – Geometry of Wound Healing.....	34
4.5 – Tissue Morphometric Data	36
4.5.1 Abnormal Tissue data	36
4.5.2 Collagen Deposition.....	37

CHAPTER 5 – CONCLUSIONS	38
APPENDIX A: PREPARATION OF SLURRY	39
APPENDIX B: RANDOMIZATION OF MATRIX IMPLANTATION	40
APPENDIX C: ASSIGNMENT OF MATRIX IMPLANTATION	41
APPENDIX D: IMAGE ANALYSIS	42
APPENDIX E: CONDITION OF TISSUE EXTRACTIONS	44
REFERENCES	45

ACKNOWLEDGEMENTS:

I would like to thank Professor Ioannis Yannas, for supporting and guiding me through this project. His teachings and advice as a thesis supervisor and professor have made this project what it is, and has helped me to become a better scientist and to communicate more clearly. I would also like to thank Brook Hill, my mentor and friend, without whom I would not have had this thesis project. I cannot thank him enough for his patient guidance, constant encouragement, and for going out of his way in volunteering so much of his time and energy to help me. Dr. Robert Marini has given me invaluable advice and ideas on my surgical protocol, and trained me in surgical technique and procedure from the ground up.

I owe an incredible debt to the people who enabled me to actually conduct the research: Ms. Katie Madden, for being so incredibly patient, helpful, and supportive of me during the many hours in the E25 Animal Facility — without her, there was simply no way I could have performed all the animal surgeries. Mr. Camille Francois, an extremely talented histologist at the VA hospital, for making my slides and doing the stains. Professor Myron Spector, for setting me up with Mr. Francois and for bringing the slides back to MIT from the VA hospital. Mr. Peter Morley of the MIT Central Machine Shop, for sharpening my curettes. Brendan Harley, for letting me use his slurry, helping me with all my questions, and for being very kind about letting me take up so much lab space. Mrs. Lorraine Rabb, for bearing with me as the expenditures mounted and for helping me with the logistical hurdles. Professor Carol Livermore, for letting me use her laboratory's microscope and Sunghwan Jung, for showing me how to use it.

I would also like to extend my appreciation and apologize to the experimental rats that were used in this experiment; I hope that the contribution to the scientific world, and the educational experience I gained, will be worthy of their sacrifice.

Finally, I would like to thank my friends and family for their support, and for their encouragement and forbearance as I worried about the completion of my thesis. I would like to especially thank Hangyul Chung, who was there every step of the way. The source of greatest happiness is to realize that I have the fortune of such wonderful companionship in life.

CHAPTER 1 – INTRODUCTION

1.1 – Renal Trauma

Every year in the United States, there are approximately 60 million incidences of trauma [1]. Renal trauma accounts for approximately 3% of all trauma admissions, or 1.8 million cases, and is implicated in approximately 10% of all patients with abdominal trauma [2]. The kidney can be injured through sources of penetrating trauma, such as gunshots and stab wounds, or through sources of blunt trauma, such as motor vehicle injuries and falls.

Of the five different grades characterizing the degree of the injury, all but the worst grade, Grade V, can usually be treated non-surgically [3]. Surgery is indicated, however, for vascular injury, shock, and expanding or pusatile hematomas [4]. Additionally, relative indications for surgery include devitalized renal segments, persistent extravasation, and loculated collections, as well as delayed diagnosis of arterial injury or segmental arterial injury [5]. Injuries that result in nonviable tissue resolve more quickly when the nonviable tissue is removed, which allows reconstruction to occur. As such, reparative surgical procedures are performed on about 60% of the patients operated on for blunt trauma and on 73% of those operated on for penetrating trauma [6].

The reparative surgery involves a midline laparotomy to first establish proximal control of the renal artery and vein, followed by attainment of renal exposure. With the capsule preserved as much as possible, the devitalized tissue is debrided, and bleeding vessels are sutured or controlled by electrocauterization. If possible, the defect in the parenchyma is approximated; when full approximation is not possible, the open defect can be covered using the capsule or an omental flap. In addition, Gelfoam bolsters can be used to approximate the capsule, or a vicryl mesh or peritoneal graft may be used to cover the defect [7]. Because total nephrectomy results in an increased risk of future renal failure of the remaining kidney, it is used minimally, with partial nephrectomy and attempted renal repair being the preferred surgical treatments.

1.2 — In Vivo Tissue Regeneration: Prior Art

Most adult mammalian organs heal irreversibly after excessive trauma or chronic insults injure the non-regenerative stroma of the tissue. That is, the tissue response to injury is to achieve closure by means of repair, rather than regeneration of functional tissue. In mammalian skin, for example, wounds are closed by the contraction of the wound site and the formation of epithelialized scar [8] instead of the non-regenerative dermis. The scar tissue lacks the full functionality of normal skin, lacking appendages such as nerve endings, sweat glands, and hair follicles.

Much recent work has focused on the use of collagen-glycosaminoglycan (GAG) matrices to induce the regeneration of tissue by preventing contraction and scarring of wounds [9]. A degradable matrix, composed of 98% type 1 bovine collagen and 5% chondroitin-6-sulfate, was fabricated to have specific pore diameters and cross-linking densities. This matrix, when applied to full-thickness skin defects, resulted in the formation of neoderms that was histologically identical to normal dermis, although skin appendages were not formed.

1.3 — Renal Tissue Engineering: Background and Prior Art

Compared to organs such as skin, the kidney is an extremely complex organ, with complicated anatomical and physiological architecture. The kidney is capable of compensatory growth, where the excision of one kidney increases the functional mass of the remaining kidney [10]. At the site of the excised kidney, however, the prevailing understanding is that the growth of new nephrons does not occur. Following parenchymal injury, scar formation and contraction, rather than regeneration, occurs. This is shown in the wound site in Figure 1.1.

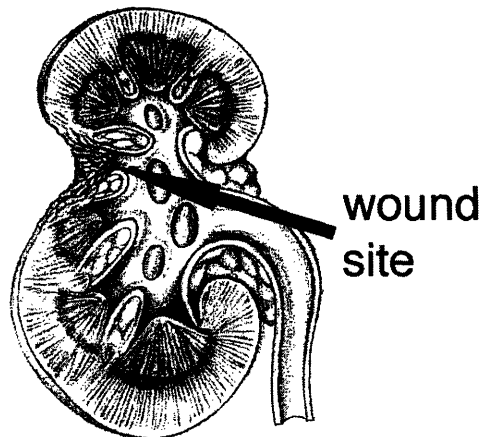


Figure 1.1: Scar formation at a renal wound site
(Source: ICON Learning Systems)

A study in which the outer cortex was destroyed without injury to the glomeruli in the basement membrane demonstrated that the capillary side of the basement membrane was repopulated by endothelial cells, and the epithelial was populated by podocytes [11,12]. Another study demonstrated that functional renal tubules could be regenerated following acute tubular cell necrosis only if the basement membrane was not ruptured [13,14].

The goal of renal tissue engineering is thus to induce regeneration after the non-regenerative stroma (i.e. parenchymal cells and glomeruli) is destroyed. A comprehensive review of the literature pertaining to induced regeneration shows that inhibition of contraction is necessary, although not sufficient, to induce synthesis of non-regenerative tissues in skin and peripheral nerves [15]. If the healing mechanism of the kidney is similar to that of skin and nerves, contraction should first be inhibited in order to achieve regeneration by the use of an extracellular matrix.

1.4 — Goals of the Current Study

A major goal of this study was the exploration of a new surgical protocol for future studies of the spontaneous healing and induction of regeneration of kidney tissue.

Accordingly, it was important to determine if the surgical protocols employed could create wounds that were reproducible from one animal to the next. Because renal tissue is a fairly elastic material with significant “springback”, a relatively unusual surgical technique had to be employed to generate wounds that had reproducible size from animal to animal. Without wounds of consistent size, it is not possible to initiate a quantitative study of the geometry of healing, a key requirement in studies of induced regeneration of organs.

The design of the surgical technique and experimental model is based upon, and seeks to improve, the methodologies used in a previous study by Brook Hill; his study tested the hypothesis that a collagen-GAG matrix would inhibit wound contraction and scarring, and induce regeneration of renal tissue after excisional injury [16]. Hill demonstrated that the implantation of collagen-GAG matrices in cylindrical defects made in the rat kidney significantly decreased scarring and collagen deposition, but failed to decrease wound contraction or induce regeneration. He suggested that the study was insufficiently powered, given the large variances in the data, for both contraction and regeneration analyses. The current study increased the power of the data by creating four wounds on each kidney, rather than two, making possible a larger sample size for a given number of animals.

In addition, the cylindrical wounds completely transected the kidney, as shown in Figure 1.2.

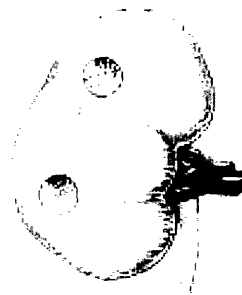


Figure 1.2: Cylindrical wounds used in a previous study

These cylindrical wounds injured the arcuate arteries that provide blood to the kidney tissue. The arcuate arteries pass between the cortex and medulla in a horizontal

plane, roughly 3 mm below the parenchymal surface (Figure 1.3). The cylindrical wound damaged these arteries in a random fashion, resulting in an uncontrolled variable in the form of secondary tissue injury in regions deprived of blood flow.

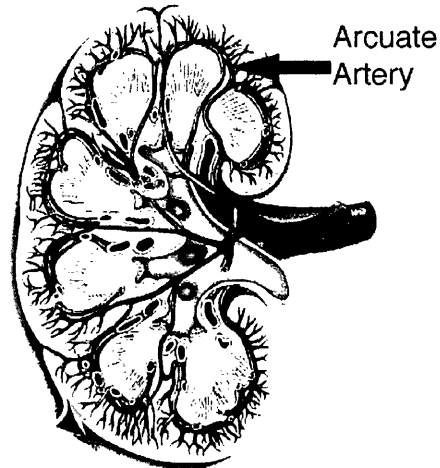


Figure 1.3: Location of arcuate arteries in the kidney

(Source: www.owensboro.kctcs.edu)

This study sought to address these limitations of the surgical model used by Hill by creating reproducible hemispherical wounds that did not extend deep enough to injure the arcuate arteries.

CHAPTER 2 – MATERIALS AND METHODS

2.1 – Matrix Fabrication

Collagen-glycosaminoglycan slurry was prepared accordingly to previously developed protocols (Appendix A). 5 mL of the slurry was poured into three aluminum dishes (Product #08-722, Fisher Scientific items) with diameters of 55 mm, and wall thickness of 0.5 mm (Figure 2.1). The dishes were chosen for their perfectly smooth surface, and for the high heat conductivity of aluminum ($k = 237 \text{ W/m}\cdot\text{K}$), which allows for uniform and predictable heat transfer from the dish to the slurry.

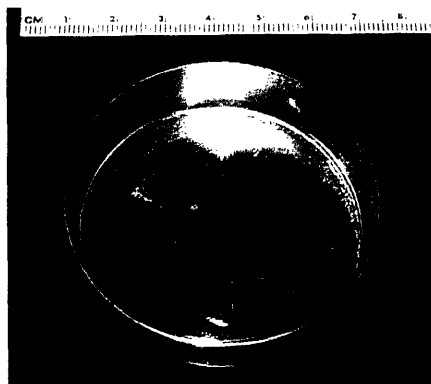


Figure 2.1: Aluminum mold for matrix fabrication

A vacuum-assisted freeze dryer (Genesis model, Vertis) was set to -40°C , and the first dish containing slurry was placed inside. After visual confirmation that the slurry had frozen completely, the freeze dryer was set to -30°C ; once the temperature was within 0.2°C of -30°C , the second dish was inserted. Again, after the slurry was confirmed to have frozen completely, the freeze dryer was set to -20°C , and the third dish was inserted.

After 30 minutes had elapsed after the insertion of the third dish, a vacuum was pulled inside the freeze dryer. The freeze dryer was then set to 0°C , and all three batches of slurry were left in the dryer overnight. The following day, the oven slowly warmed to

room temperature, and the vacuum was released. The matrices were then removed from the dishes in the form of a matrix “wafer”.

Because the matrix wafer is very fragile, it is very difficult to reliably and precisely cut out cylinders. The stainless steel bit from a 3-mm dermal biopsy punch (Miltex Instrument Co.) was attached to a Dremel tool (Model 395 Type 5) as shown in Figure 2.2.



Figure 2.2: Biopsy punch attachment to Dremel

The Dremel was mounted on a drill press assembly, and was run at 30,000 RPM. With the matrix wafer held in place with one hand, the Dremel was lowered to cut out small matrix cylinders, roughly 3mm in diameter and 1-2 mm in height. 22-25 matrix cylinders were cut out from each of the three wafers, and were placed in labeled glass vials.

The vials containing the matrix cylinders were placed in a dehydrothermal oven (IsoTemp Model 201; Fisher Scientific) and heated for 12 hours at 105°C. After heating, the matrices were immersed in 100% ethanol for 1 minute, then in 70% ethanol for 1 minute, followed by two 1 minute immersions in separate 40% ethanol solutions, before being rinsed in sterile phosphate buffered saline solution (PBS). The ethanol rinses were performed before rewetting with PBS to preserve the microstructure of the matrix. The matrices were stored in vials of sterile PBS at room temperature.

The matrices were consistently 3.0-3.0 mm in diameter, with a thickness of 1.0-2.0 mm. As expected, increasing the freezing temperature increased the average pore diameter (Table 2.1).

Freezing Temperature	DHT	Average Pore Diameter (μm)
-20°C	100° for 12 hours	182.0 +/- 4.6
-30°C	100° for 12 hours	133.2 +/- 8.5
-40°C	100° for 12 hours	100.6 +/- 5.4

Table 2.1: Matrix Properties

During the course of the experiment, the vial containing the matrices frozen at -30°C was very visibly contaminated by fibrous debris from the paper-based lining in the cap of the vial. Because this contamination was not controlled for, and the identity of the contaminant is not known, all data resulting from implantation of the matrix frozen at -30°C will not be analyzed in this study.

2.2 — Experimental Paradigm

The experimental protocol was reviewed and approved by the MIT Committee on Animal Care (CAC) prior to the purchase of animals. Twenty adult male Wistar-Hanover rats (*Rattus norvegicus*, Charles River Laboratories, Wilmington, MA) were obtained, and were housed in the MIT Animal Facility (Figure 2.3). Each rat was numbered sequentially from 1-20.



Figure 2.3 Male Wistar-Hanover rat

Two semi-spherical wounds were created in each hemisphere of each rat's left kidney, as shown in Figure 2.4, for a total of four wounds labeled a-d for each kidney.

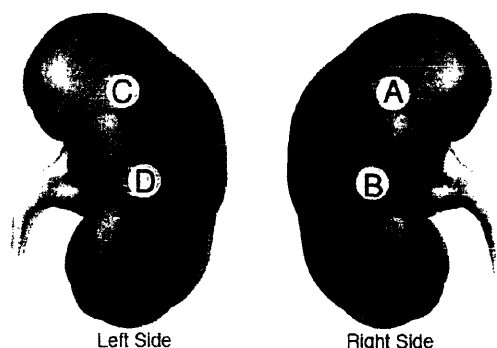


Figure 2.4: Labeling system for wounds

Three of these holes were implanted with one of the three types of matrices frozen at temperatures of -40°C , -30°C , and -20°C . The fourth wound remained untreated to serve as the negative control.

2.3 — Implantation Surgery Protocol

Fifteen to thirty minutes before surgery, the animal was intraperitoneally injected with 80 mg/kg ketamine (Fort Dodge Animal Health) and 10 mg/kg xylazine (Phoenix Scientific Inc.) to achieve operative anesthesia. Additionally, 1.5-2.05% in 100% O_2 of vaporized isoflurane (Baxter Pharmaceutical Products Inc.) was given to the animal during the surgery .

The sterile surgical procedure to attain exposure of the left kidney was performed exactly as described in detail in the previous study by Hill [17]. With the animal placed in a right lateral decubitus position, a 4-5 cm longitudinal incision was made 2-4 cm lateral to midline, parallel to the spinal column. This incision cut through the skin and the underlying fascia; the body wall was then cut with Metzenbaums, and the left kidney was exposed as shown in Figure 2.4.



Figure 2.4: Left kidney with intraperitoneal fat

The fat surrounding the kidney was carefully removed with the forceps and Metzenbaums, leaving the kidney capsule and nearby vasculature unharmed (Figure 2.5).

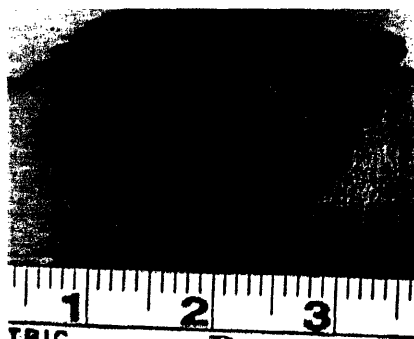


Figure 2.5: Kidney with intraperitoneal fat

With the kidney thus clearly exposed, a 1 mL insulin syringe (Ultra-Comfort Monoject Insulin Syringe, Kendall) was used to inject a 0.09% saline solution (0.9% NaCl irrigation solution; Baxter) into the sub-capsular space (Figure 2.6) along the midline of the kidney, forming a “welt” on the surface of the capsule.



Figure 2.6: Injection of saline in subcapsular space

A #15 surgical blade was used to make an incision across this “welt”. The underlying parenchyma was not cut by the blade because the capsule was separated from the tissue by the entrapped liquid.

A pair of micro-dissecting scissors (Product H50-711, Harper, Inc.), as shown in Figure, was used to extend the capsular incision longitudinally for 1.0-1.5 cm, using a pair of curved microforceps (Product RS-5137, Roboz, Inc.) as a groove director.

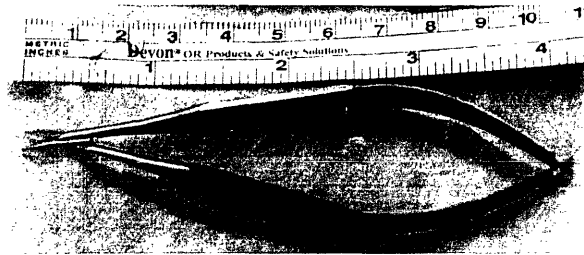


Figure 2.7: Micro-dissecting scissors

As the incision was made, the natural tension of the capsule was relieved, and the capsule thus retracted laterally (Figure 2.8).



Figure 2.8 Capsule of kidney

The microforceps were then gently inserted under the capsule, and slid down roughly 75% to the surface of the parenchyma to separate the capsule from the parenchyma. With the parenchymal surface thus exposed, 0.1-0.3 mL of sterile filtered India Ink (Product # 500200N, Permark, Inc) was injected into the sub-capsular region, coating the entire parenchymal surface. The kidney was left undisturbed for 3-5 minutes

to allow the ink to dry; care was given to ensure that the kidney did not dry out excessively (Figure 2.9).



Figure 2.9: Kidney covered in India ink

A 3mm diameter open-faced curette, as shown in Figure 2.10 (RS-6356, Roboz Surgical Instrument Co, Inc.) was sharpened by diamond lapping by the MIT Central Machine Shop. This curette was used to carefully scoop out four hemispherical wounds on the surface of the parenchyma.



Figure 2.10: 3mm open-faced curette

Two wounds were created in each hemisphere of the kidney; one wound was created near the anterior pole, while the second wound was created in a more posterior location. For Rats #2-9, the curette was carefully inserted into the sub-capsular space by what will be referred to in this paper as “Technique A”. For Rats #10-20, “Technique B” was used, wherein the incision in the capsule was sufficiently lengthened to allow the capsule to be completely laterally retracted. The head of the curette could then be placed unencumbered on the surface.

The face of the curette was oriented parallel to the surface of the parenchyma (Figure 2.11), and the curette was rolled back and forth, in place, such that the edge of curette incrementally cut into the parenchymal surface. As little force as possible was applied to surface, to avoid traumatic injury and deformation of the kidney.

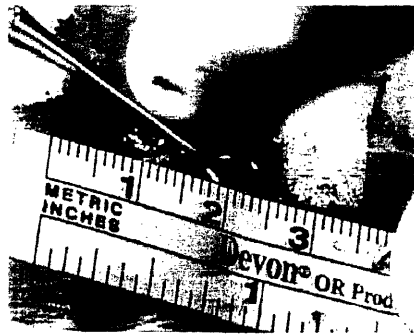


Figure 2.11: Creation of hemispherical wound with curette

Once the curette head was able to rotate approximately 45° into the kidney in both directions, the curette was turned around completely in one direction to excise the tissue. (Figure 2.12). Although the kidney is heavily vascularized, this surgical protocol intentionally avoided injury to the arcuate arteries, which transport much of the blood to the organ, and hemostasis of the wound site was achieved in 5-10 minutes by the placement of cotton-tipped applicators and moistened surgical gauze over the wound.



Figure 2.12: Excision of tissue from wound

The excised tissue bits, shown in Figure 2.13, were stored in 10% neutral buffered formalin (Protocol Formalin, CAT# 245-684, Fisher Scientific Company) for later analysis.

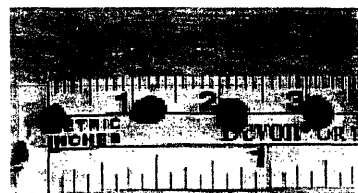


Figure 2.13: Excised tissue samples

Three of the four wounds that were created were implanted with one of the three types of matrices (Figure 2.14), with the fourth wound remaining untreated to serve as the control. The specific matrix that was implanted in a given wound was determined as outlined in Appendix B.



Figure 2.14: Matrices implanted in wounds

Appendix C lists the characteristics of the matrices assigned to each wound. Two rats were designated as internal controls, and were sacrificed immediately after surgery; this control group served to ensure the accuracy with which the original wound characteristics could be measured post-operatively, and to ensure proper wound geometry.

The capsule proved to be too fragile to suture closed using 10-0 suture, so after the matrices were implanted, the capsule was very gently pulled back above the wound site, where it remained over the wound site due to friction and adhesive effects of the blood (Figure 2.15).



Figure 2.15: Capsule covering the wound site

After all matrices were implanted and covered, the kidney was very gently placed back in the body cavity, and the body wall was closed using 4-0 Vicryl absorbable sutures (Ethicon, Inc.) using a simple interrupted suturing pattern. The outer skin was closed using Michel clips.

2.4.— Post-operative care

After the surgery was completed, the animals were taken off of isoflurane, and were injected with 0.10 mg/kg buprenorphine (Buprenex, Reckitt & Coleman) intramuscularly for pain relief. Animals were housed two per cage, and were inspected daily for health and well-being at least ten days after surgery. In rare cases when staples were sufficiently loosened or removed such that there was no longer complete apposition of the wound, the wound was irrigated with disinfecting solution and re-stapled.

2.5 — Animal Sacrifice and Kidney Removal Surgery

Four weeks after the implantation surgery, each animal was sacrificed via CO₂ asphyxiation. The left kidney was exposed using the same surgical procedure as the implantation surgery. Due to the formation of fibrous connective tissue around the kidney, the liver, intestine, and additional fat were found tightly attached to the kidney (Figure 2.16). These attachments were very carefully removed with the microscissors and microforceps.



Figure 2.16: Kidney four weeks post-operatively

The kidney was then removed, and the anterior pole was marked with non-absorbable suture. All kidneys were photographed at this time (Figure 2.17), and were fixed in 10% formalin.

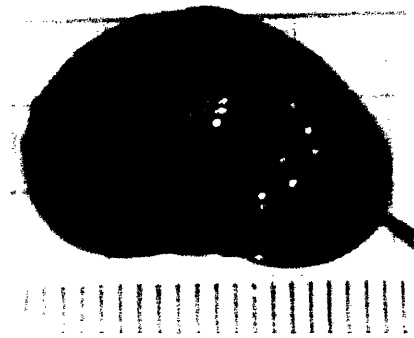


Figure 2.17: Kidney removed from animal four weeks post-operatively

2.6 — Morphology

2.6.1 Gross Morphology

The excised tissue samples taken from the wounds, after being fixed in 10% formalin, were placed on engineering graph paper, such that the exterior surfaces were all facing up, as shown in Figure 2.18.

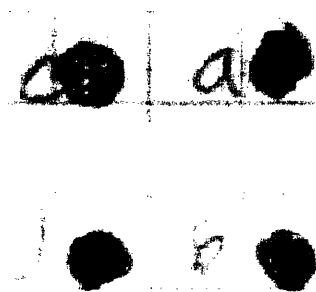


Figure 2.18: Excised tissue, fixed in 10% formalin

The excised tissue samples were photographed using a 2.0 megapixel digital camera (PowerShot S200, Canon, Inc.) under ambient room light conditions. The surface

areas were then measured as described in Appendix D, to provide an indirect estimation of the surface area of the original wound. The fixed experimental kidneys were also similarly photographed and analyzed to provide an indication of the surface area of the wound after 40 days.

2.6.2 Histology and Immunohistology

Each kidney was first manually dissected longitudinally using a #10 scalpel blade. For each wound of the half-kidney, two transverse slices (perpendicular to the flat side created by the longitudinal slice) were made; one slice was made to pass through the diameter of the wound, and the other slice was made parallel and about 3 mm away from the first slice. The section was then placed in a labeled histological cassette, and after the tissue was processed and embedded, the slides were stained with Masson's trichrome and Δ -smooth muscle actin (Δ -SMA) immunostaining. The Δ -smooth muscle actin staining protocol has been described in previous literature [17]

2.6.3 Image Analysis of Histological Slides

Images of histological slides were captured using a Nikon compound microscope (Nikon Optiphot) attached to an analog camera assembly (camera: Nikon FX-35WA, power supply: AFX-11A), using 35mm ASA 400 film (Kodak Max 400). In addition, to calibrate the microscope to size, a standard hemacytometer (Bright-Line Hemacytometer; Recihert, Inc.) with grids of known size (e.g. 25, 50, 100, 250, and 1000 μm) was photographed.

Film was developed and digitized to jpeg format by Ritz Camera (Cambridge, MA). The images were then analyzed for scarring and collagen deposition according to the protocol detailed in Appendix D.

Each type of matrix was stained with Mayer's Hematoxylin (Sigma-Aldrich, St. Louis, MO) to enhance visibility of the matrix architecture, and was photographed and analyzed under 10x magnification.. The diameters of five random pores were measured and averaged to yield the average pore diameter.

2.6.3 Statistical Methods

Statistical analysis of the contraction, scarring, and collagen deposition data was conducted using Microsoft Excel. The values for each treatment condition were averaged, and both paired, one-tailed t-tests and two-sample (unequal variance) one-tailed t-tests were used to determine whether the treated condition was significantly different from the untreated condition.

CHAPTER 3 – RESULTS

3.1 – Surgical and Post-Operative Outcomes

All animals tolerated the procedure well. No animals died unintentionally, and complications were not observed. Rat #1 was sacrificed immediately after the operation because of excessive unintentional injury to the kidney; data from this kidney was not collected. A small piece of gauze was left in the body cavity of Rats #6 and #7, but this did not have a noticeable effect on the final state of the kidney or the post-operative health of the rat. Several animals scratched and chewed the skin staples off their wounds, while others exhibited auto-mutilatory behavior resulting in superficial scratches. After disinfecting the wound site, the staples were reattached, and no further complications arose for these animals.

3.2 – Reproducibility of Surgical Protocol

The reproducibility of the wound was determined by measurement of the mass of the “tissue extraction” that was removed when the wound was created (shown earlier in Figure 2.19).

The masses of the tissue extractions, as well as their geometric conditions, are presented in Appendix E. The reproducibility of the wounds varied according to the surgical technique, as shown in Table 3.2; as described in Section 2.3, Technique A entailed inserting the curette under the capsule, while Technique B entailed peeling back the capsule prior to the cutting of the wound.

Technique	Number of Rats	Average Mass (g)	Standard Dev. (g)
A+B	19	14.11	5.28
A	8	14.68	6.98
B	11	13.7	3.62

Table 3.1: Reproducibility of wounds by technique

The average values for the two techniques do not significantly differ ($p=0.48$ for a two-sample, unequal variance, two-tailed test between Techniques A and B), but Technique A had a standard deviation that was 1.93 times greater than that of Technique B, indicating that there was more variation in the wounds in Technique A.

3.3 — Geometry of Healing

3.3.1 Description of Wound Site

Figure 3.1 illustrates a representative healed wound four weeks after the matrix implantation surgery. The wound site was characterized by two perimeters. Outside the original wound site was a greater area of a crater-like depression, which will be referred to as the “lacuna” area (the area inside it will be referred to below as L), shown by the white perimeter in the figure. Inside this lacuna was a distinct, often darker, area that was marked by a sudden indentation; this area will be referred to as the “wound” area (referred to below as W), and is shown by the yellow perimeter in the figure.

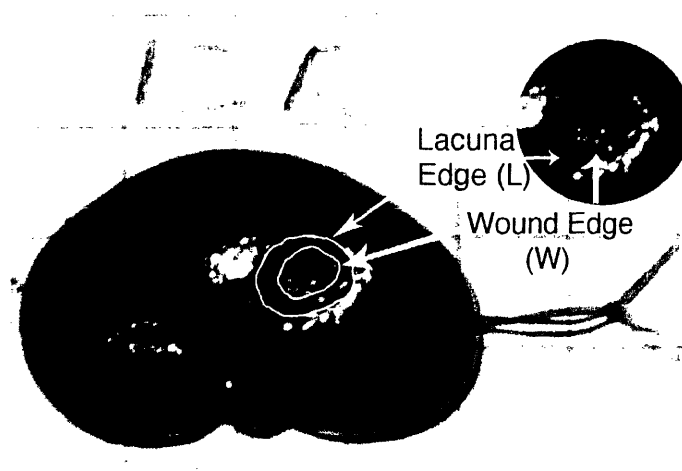


Figure 3.1: Wound site geometry, indicating wound and lacuna perimeters

3.3.2 Wound Area

The original and final wound areas, W_o and W , respectively, were measured, and the change in wound area following healing, $W - W_o$, was calculated by finding the difference between the original and final wound area as shown in Figure 3.2. This measure indicates the extent to which the original wound perimeter was displaced inward as a result of the healing process.

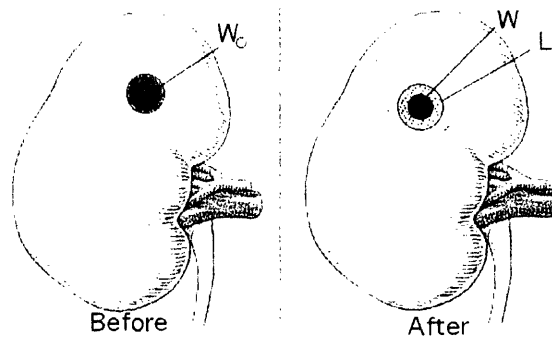


Figure 3.2: Illustration of the original wound (W_o), healed wound (W), and lacuna (L) areas

The change in wound area, $W - W_o$, for each of the treatment conditions was compared to that for the corresponding control (untreated) wound using both a paired and unpaired (two-sample), one-tailed t-test; the data can be seen in Table 3.2. "Paired" data are taken from two wounds in the same kidney (same animal) and are therefore free of factors related to animal-to-animal variability. "Unpaired" data are those taken from wounds in the entire animal population and include all factors that relate to animal-to-animal variability.

Rat #	W-W ₀ (mm ²)		
	Matrix A	Matrix B	Control (no matrix)
2	-3.98	-6.24	-1.36
3	-5.13	-4.03	-0.17
5	-0.34	-1.32	-0.57
7	-6.66	-6.74	-5.02
9	-	-5.56	-4.03
10	-4.67	-	-0.94
13	-5.14	-3.50	-1.10
14	-9.29	-1.03	-2.61
15	-4.49	0.01	-0.11
17	-0.22	-4.94	0.03
18	-4.19	-4.17	-3.59
19	-4.31	-3.73	1.01
Average	-4.40	-3.75	-1.54
Standard Dev.	2.54	2.18	1.86
Unpaired p-value (significant if p<0.05)	0.003	0.008	
Paired p-value (significant if p<0.05)	0.0006	0.001	

Table 3.2: Effect of matrix implantation on wound areas

The unpaired analysis shows that both Matrix A and Matrix B had significantly decreased W, the area of the healed wound, compared to the untreated control. The paired analysis led to a similar conclusion. In both cases, the level of significance was measured by the p-value, the probability that the observed differences were due to chance (i.e., random changes in experimental parameters). The p-values were always less than 0.05 (5%), indicating a probability smaller than 5% that the observed differences were due to chance. There was no significant difference between the effects of Matrix A and B (p=0.93). The paired analyses yielded lower p-values than the unpaired analyses; using the paired analysis, we can ascribe a greater degree of significance to the effects of Matrix A and B than if we used only the unpaired analysis.

3.3.3 Lacuna Area

The total lacuna area, L , was measured as shown earlier in Figure 3.2; the lacuna area, which is roughly equal to or larger than the original wound area, reflects a distortion of the tissue surrounding wound site.

The change in lacuna area for each of the treatment conditions was compared to that for the corresponding control (untreated) wound using both a paired and unpaired (two-sample), one-tailed t-test; the data can be seen in Table 3.3.

Rat #	L-L ₀ (mm ²)		
	Matrix A	Matrix B	Control (no matrix)
2	8.74	10.52	16.50
3	8.59	6.22	9.51
5	10.12	5.12	22.37
9	-	5.92	14.82
10	4.26	-	10.20
11	-	5.68	16.01
14	15.30	17.56	18.11
18	9.01	10.62	16.70
Average	9.34	8.81	15.53
Standard Dev.	3.55	4.50	4.16
Unpaired p-value (significant if p<0.05)	.006	.005	
Paired p-value (significant if p<0.05)	.006	.005	

Table 3.3: Effect of matrix implantation on lacuna areas

The unpaired ($p=0.006$) and paired analysis ($p=0.005$) revealed that both Matrix A and B significantly decreased the size of the lacuna, as compared to the untreated wound, although there is no significant difference between the effects of Matrix A and B ($p= 0.19$). The paired analysis yielded p-values that were the same as the p-values from an unpaired analysis for both matrices.

3.4 — Tissue Morphometric Data (Histological Data)

3.4.1 Abnormal Tissue Area

Figure 3.3, a cross-section of a representative wound stained with trichrome, illustrates the formation of abnormal tissue, referred to below as AT, around and below the wound site. The amount of abnormal tissue serves as an indication of the extent of injury around the wound.

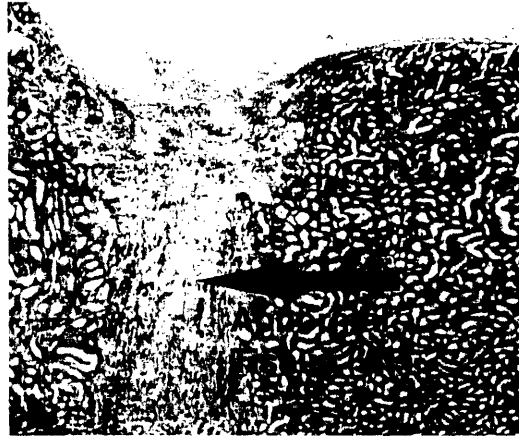


Figure 3.3: Abnormal Tissue (AT) around the wound site

The location of the cross section is schematically illustrated in Figure 3.4.

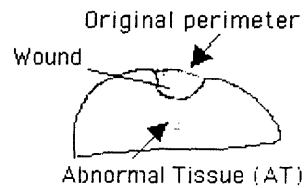


Figure 3.4: Location of Abnormal Tissue (AT) in context of the entire cross-section

The area of abnormal tissue in each of the treatment conditions was compared to the abnormal tissue in the corresponding control (untreated) wound using both a paired and unpaired (two-sample), one-tailed t-test; the data can be seen in Table 3.4.

Rat #	AT (mm ²)		
	Matrix A	Matrix B	Control (no matrix)
2	0.748	0.535	0.444
3	0.451	0.597	0.641
5	0.458	0.632	0.419
6	0.756	0.490	0.539
7	0.248	0.424	0.341
9	0.691	0.493	0.298
10	0.084	0.103	0.164
11	0.083	0.441	0.148
13	0.427	0.276	0.433
14	0.262	0.104	0.355
15	0.611	0.730	0.675
16	0.644	0.264	0.582
Average	4.55E-01	4.24E-01	4.20E-01
Standard Dev.	2.43E-01	2.00E-01	1.70E-01
Unpaired p-value (significant if p<0.05)	0.34	0.48	
Paired p-value (significant if p<0.05)	0.25	0.47	

Table 3.4: Effect of matrix implantation on abnormal tissue (AT) area

Neither the paired nor the unpaired analysis reveal ($p \geq 0.25$) a significant effect of either matrix on the amount of abnormal tissue surrounding the wound site. There was also no significant difference between the effect of Matrix A and B on the amount of abnormal tissue that formed ($p=0.37$).

3.4.2 Collagen Deposition

Figure 3.5, a cross-sectional view of a representative wound stained with trichrome, illustrates the collagen deposition, referred to below as CD, at the wound site, which serves to characterize the healing response at the wound site.

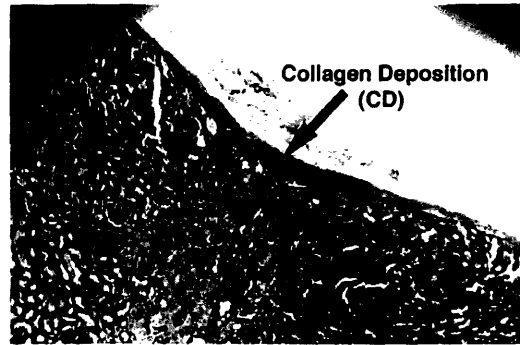


Figure 3.5: Collagen Deposition (CD) at the wound site

The location of the wound in Figure 3.5 is schematically illustrated in Figure 3.6.

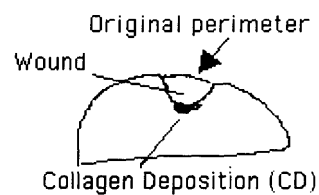


Figure 3.6: Location of Collagen Deposition (CD) in context of the entire cross-section

The areas of collagen deposition (CD) in the treatment conditions were compared to the collagen deposition in the control (untreated) wound using both a paired and unpaired (two-sample), one-tailed t-test; the data can be seen in Table 3.5.

Rat #	CD (mm ²)		Control (no matrix)
	Matrix A	Matrix B	
2	2.31E-02	5.50E-04	1.54E-02
3	1.10E-02	6.55E-03	1.67E-02
5	6.44E-03	1.17E-02	2.77E-02
6	1.08E-01	2.13E-02	1.07E-02
7	1.35E-02	1.71E-02	2.28E-02
9	6.32E-03	1.05E-02	2.09E-02
10	2.43E-02	1.54E-04	2.31E-03
11	7.12E-03	1.94E-02	1.41E-02
13	1.06E-02	7.44E-03	5.00E-04
14	7.92E-03	1.99E-03	0.00E+00
15	3.12E-02	1.03E-03	1.07E-02
16	3.09E-02	1.13E-02	2.70E-02
18	4.07E-02	8.56E-03	3.33E-02
Average	2.47E-02	9.04E-03	1.55E-02
Standard Dev.	2.74E-02	7.13E-03	1.07E-02
Unpaired p-value (significant if p<0.05)	0.14	0.04	
Paired p-value (significant if p<0.05)	0.14	0.02	

Table 3.5: Effect of matrix implantation on area of collagen deposition (CD)

Both the unpaired and paired analyses indicated that Matrix A did not significantly decrease collagen deposition compared to the untreated wound (p=0.014 for both paired and unpaired t-tests). Both the unpaired and paired analyses indicated that Matrix B significantly decreased collagen deposition by 41.7%, as compared to the untreated wound. The paired analysis revealed a slightly greater significance (p=0.02) than the unpaired analysis (p=0.04).

CHAPTER 4 – DISCUSSION

4.1 – Summary of Matrix Effects

Matrix A, which was freeze-dried at -20°C and cross-linked by baking for 12 hours at 100°C , had a pore size of $182.0 \pm 4.6 \mu\text{m}$. The implantation of Matrix A in the hemispherical wound did not significantly alter the amount of abnormal tissue ($p=0.25$) or collagen deposition ($p=0.14$) at the wound site, as compared to the untreated control. However, Matrix A significantly decreased the area of both the healed wound ($p=0.003$) and the lacuna, a region of greater depression around the wound ($p=0.006$).

Matrix B, which was freeze-dried at -40°C and cross-linked by baking for 12 hours at 100°C , had a pore size of $100.6 \pm 5.4 \mu\text{m}$. The implantation of Matrix B did not significantly alter the amount of abnormal tissue ($p=0.47$) at the wound site, but significantly decreased collagen deposition ($p=0.04$) as well as the area of both the healed wound ($p=0.008$) and the lacuna ($p=0.005$).

4.2 – Paired versus Unpaired Statistical Analysis

Both paired and unpaired t-tests were used to determine the significance of the effects of the matrices. In the paired analysis, wounds from the same kidney (animal) were compared to each other, while in the unpaired analysis, the population of experimental wounds was compared to the population of control wounds irrespective of which kidney the wound was from. The paired analysis thus eliminates animal-to-animal variability, and is expected to better reveal significance, in the form of having a smaller p-value. The p-value is the probability that the difference between the two groups is due to chance. In this study, if the p-value was or below 0.05, the difference between two groups was considered significant. The effect of matrix implantation on the final wound area was more significant when analyzed using a paired analysis instead of an unpaired analysis. For all other assays, the paired analysis demonstrated the same significance, or a marginally greater significance, as compared to the unpaired analysis.

4.3 — Reproducibility of Surgical Protocol

The surgical protocol used in this study led to the generation of wounds with highly reproducible initial area. The standard deviation of time-zero wound areas, measured using the excised tissue flaps, was 12%. This compares favorably to the standard deviation of time-zero surface wound areas in Hill's study, which was 19% of the measured area.

The average wound areas for the two techniques used in this study, Technique A and B do not differ significantly ($p=0.48$), but Technique B produced wounds with much less variability in their areas. The standard deviation of wounds made with Technique B was 52% of the standard deviation for Technique A. In Technique A, the curette was inserted under the capsule to create the wound. The blood that accumulated under the capsule precluded visual monitoring of the wound creation. In Technique B, the capsule was peeled back, and the curette head and wound site could be easily seen. Technique B resulted in increased reproducibility because the generation of wounds could thus be better monitored.

4.4 — Geometry of Wound Healing

Upon healing, the hemispherical wound exhibited contraction of the wound perimeter, and also produced a "lacuna," a crater-like area of depression surrounding the original wound site, often with a slight elevation at the perimeter. Implantation of both Matrix A and Matrix B significantly altered the geometry of wound healing, as the matrices decreased the area of the wound, W , and the lacuna area, L . Matrix A decreased the wound area by 26%, and the lacuna area by 27%. Matrix B decreased the wound area by 41% and the lacuna area by 43%. The difference between the effects of Matrix A and B on the wound area ($p=0.93$) and on the lacuna area ($p=0.14$) were not significant.

The previous study by Hill did not lead to a conclusion on the effect of treatment with matrices on contraction [19]; the surgical protocol in that study resulted in unpredictable tissue damage that was not controlled, and the variance of the data was too large to demonstrate a significant effect of the matrices. The hemispherical wounds

created in the current study avoided damage to the arcuate arteries, reducing variability in the severity of secondary injury; the reduction in variability was large enough to enable this surgical model to reveal a statistically significant effect of matrices on wound geometry.

A paired analysis, where each experimental wound was compared to the untreated control wound on the same kidney, revealed a higher degree of significance than the unpaired analysis for the wound in the form of lower p-values. Matrix A's paired p-value was 17% of the unpaired p-value, and Matrix B's paired p-value was 12% of the unpaired value. This indicates that the surgical protocol that created multiple wounds on the same kidney was useful in revealing significance in treatment with a matrix. Having an untreated wound on each kidney allowed a paired analysis to be performed, which eliminated animal-to-animal variability and increased the significance of the results.

Additional analysis is needed to interpret the geometrical data to elucidate the physical mechanism of contraction and the formation of the lacuna. The complex deformation pattern that included formation of lacuna on the surface of the kidney (Fig. 3.1) cannot be readily explained without further detailed analysis. Even though the wound area (ΔW) data are consistent with wound contraction that increases in extent when one of the matrices was used, the corresponding significant decrease in lacuna area (ΔL) appears to point in the opposite direction.

In future studies a finite-element analysis should be performed to model how the hemispherical wound is deformed under the influence of low or high contractile forces that are applied at the bottom as well as at the sides of the hemispherical wound cavity. The location of the forces, and possibly a very rough measure of their relative magnitude, can be deduced from the Δ -smooth muscle actin stains, which reveal the presence, location and number of contractile cells.

In the absence of data from finite-element analysis, one conceivable model is that, when strong contraction forces are applied at the bottom of the wound, the surface of the wound "crater" splays outward, generating a lacuna. If this model is correct, a wider lacuna diameter implies higher contractile forces at the bottom of the wound. The fact that the matrices decreased the lacuna diameter would then suggest that the matrices decreased the contractile forces in the wound.

It is important to recognize the possibility that the change in wound geometry was not caused by contraction exclusively, as regeneration of new tissue may have occurred. The use of India ink to track the movement of the original wound edge failed because the ink did not adhere to the original parenchymal tissue. The ink instead either attached to the capsule or was wiped out from the kidney surface by relative movement of tissues adjacent to the kidney surface. Thus, this study cannot prove that the perimeter of the healed wound area (W) reflects the old tissue at the boundary of the original wound, as is necessary to conclude if the change in geometry is considered to be exclusively due to contraction.

Because the healed wound perimeter may instead reflect the perimeter of new, regenerated, tissue, one possible explanation for the results of this study is that the matrix reduced contraction at the bottom of the wound, causing the lacuna diameter to be smaller, but also induced regeneration, causing the wound diameter to be smaller. To test this theory, a different type of marker, or a different method of administration, should be used to permanently identify the perimeter of the original tissue.

4.5 — Tissue Morphometric Data

4.5.1 Abnormal Tissue data

The amount of abnormal tissue was measured to serve as an indication of the extent of injury to tissue around the wound. Although the paired analysis yielded lower p-values than the unpaired analysis for both Matrices A and B, neither the paired nor unpaired analysis revealed a significant effect of either Matrix A or B on the amount of abnormal tissue surrounding the wound site, with all p-values being at least 0.25, which is greater than the 0.05 necessary to indicate significance. There was also no significant difference between the effect of Matrix A and B on the amount of abnormal tissue ($p=0.37$).

The lack of significance appears in this case to be related to the excessively high values of standard deviations compared to the small average difference between areas. The area of abnormal tissue in the wound treated with Matrix A was larger than the area of abnormal tissue in the untreated wound by 8%,

It is important to note that the identity of the abnormal tissue has not been positively identified in this study. Hill has suggested that this abnormal tissue is scar [19]. However, the abnormal tissue had been selected because it was slightly lighter in color and qualitatively different in appearance; the present study has not provided evidence regarding the identity of the abnormal tissue.

If this assay is to be used in a future study, the identity of the abnormal tissue should be unambiguously determined and confirmed.

4.5.2 Collagen Deposition

Collagen deposition was measured to reflect the extent to which fibrotic tissue was synthesized in the wound. Matrix A did not significantly alter the amount of collagen deposition as compared to the untreated wound. However, the implantation of Matrix B, which has a pore diameter of 101 μm and was cross-linked for 12 hours at 100° reduced collagen deposition by 42% as compared to an untreated wound. This result supports the finding of the previous study by Hill [18], in which the implantation of a matrix with a pore diameter of 83 μm , cross-linked for 12 hours at 105° reduced collagen deposition by 52%. The data thus suggest that the treatment of a wound with a collagen-glycosaminoglycan matrix reduces the synthesis of fibrotic tissue in the injured kidney, which is a highly desirable objective with respect to the goal of achieving regeneration of functional tissue.

In this assay, a paired analysis did not offer a large improvement over an unpaired analysis. For Matrix A, the p-value was the same ($p=0.14$), while for Matrix B, the paired p-value ($p=0.02$) was slightly lower than the unpaired p-value ($p=0.04$). The fact that both paired and unpaired analyses yielded similar results suggests that the advantage of eliminating animal-to-animal variability was minimal. That is, with respect to collagen deposition, there was not much variation between animals undergoing the same wound treatment. Collagen deposition may thus be a good assay to use to reveal the effect of matrix implantation; because it is otherwise fairly constant from animal to animal (factors unique to the animal do not greatly influence the amount of collagen deposition), this assay can more easily reveal any effect of matrix implantation than assays that are more variable.

CHAPTER 5 – CONCLUSIONS

The surgical model used in this study enabled the creation of reproducible hemispherical wounds in the rat kidney that avoid injury to the arcuate vessels. The healing resulted in the contraction of the wound, and the formation of a lacuna, a crater-like depression with a raised lip, around the wound site. The implantation of collagen-glycosaminoglycan matrices with pore diameters of 101 μm and 182 μm significantly altered the geometry of the healing mechanism. The matrix with a pore diameter of 101 μm had the greatest effect on wound geometry, decreasing the lacuna area by 43% and the wound area by 41% as compared to the untreated control. The matrix with a pore diameter of 182 μm decreased the lacuna area by 37% and the wound area by 26%.

This finding is significant because it supplements the finding of an earlier study, which was not able to demonstrate a significant effect of matrix implantation on wound geometry. A finite element analysis, modeling the wound closure using data from the Δ -smooth muscle actin stained sections, should be conducted in a future study to enable the healing mechanism to be better understood.

Neither matrix significantly altered the area of a certain, unidentified, type of abnormal tissue that formed around the wound site. However, the matrix with a pore diameter of 101 μm was found to significantly decrease collagen deposition by 42%; this supports the result of a previous literature that showed that a matrix with a pore diameter of 83 μm reduced collagen deposition by 52%. The data thus consistently reveal that a glycosaminoglycan matrix can reduce the synthesis of fibrotic tissue in the injured kidney, which is a highly desirable objective with respect to the goal of achieving regeneration of functional tissue.

APPENDIX A: PREPARATION OF SLURRY

(From Hill, 2004)

1. Defrost wet Integra tendon collagen for 30-60 minutes, while simultaneously cooling the blenders to $\sim 4^{\circ}\text{C}$.
2. Fill one blender with 600 ml of 0.05 M acetic acid.
3. Pull 13.69 g of wet tendon collagen into small bits using forceps.
4. Add collagen to blender, and blend for 90 minutes on high.
5. Add 120 ml chondroitin-6-sulfate solution (0.32 g C-6-S in 120 ml 0.05 M acetic acid) over 15 minutes using the peristaltic pump.
6. Blend for an additional 90 minutes on high.
7. De-gas slurry in a vacuum flask for 10-15 minutes, and refrigerate for future use.

APPENDIX B: RANDOMIZATION OF MATRIX IMPLANTATION

Software: MATLAB, V 6.1.0.450, The MathWorks, Inc. Natick, MA

```
%Provides random order for matrix implantation  
%Roy Esaki  
%January 2004
```

```
for i=1:20
```

```
matrix_permutation(i,:)=randperm(4)
```

```
end
```

```
%This yields twenty sets of random permutations of the  
numbers [1, 2, 3, 4]  
%Each number represented a matrix or control situation as  
follows:
```

```
%1 -20 degrees
```

```
%2 -30 degrees
```

```
%3 -40 degrees
```

```
%4 control
```

```
%Within each set of permutations, the first number of the  
series represented the %matrix to be implanted in Wound A,  
the second number represented the matrix in %Wound B, and  
so on. Each of the twenty sets represented the left kidney  
from one of %the twenty experimental rats.
```

**APPENDIX C:
ASSIGNMENT OF MATRIX IMPLANTATION**

Rat Number	Matrix Condition	Rat Number	Matrix Condition
2a	Control	12a	-40°C
2b	-30°C	12b	-30°C
2c	-40°C	12c	Control
2d	-20°C	12d	-20°C
3a	Control	13a	-30°C
3b	-30°C	13b	-40°C
3c	-20°C	13c	Control
3d	-40°C	13d	-20°C
4a	-20°C	14a	-30°C
4b	Control	14b	-40°C
4c	-30°C	14c	-20°C
4d	-40°C	14d	Control
5a	-40°C	15a	-40°C
5b	-20°C	15b	Control
5c	-30°C	15c	-30°C
5d	Control	15d	-20°C
6a	-20°C	16a	-40°C
6b	Control	16b	-30°C
6c	-40°C	16c	-20°C
6d	-30°C	16d	Control
7a	Control	17a*	-40°C
7b	-40°C	17b*	-20°C
7c	-20°C	17c*	Control
7d	-30°C	17d*	-30°C
8a	-30°C	18a	-20°C
8b	Control	18b	-30°C
8c	-20°C	18c	-40°C
8d	-40°C	18d	Control
9a	Control	19a*	Control
9b	-30°C	19b*	-30°C
9c	-40°C	19c*	-40°C
9d	-20°C	19d*	-20°C
10a	Control	20a	-40°C
10b	-20°C	20b	Control
10c	-40°C	20c	-20°C
10d	-30°C	20d	-30°C
11a	Control	*17 and 19 were sacrificed immediately	
11b	-20°C		
11c	-40°C		
11d	-30°C		

Table B.1: Description of treatment condition for wounds

APPENDIX D: IMAGE ANALYSIS

Software:

•ImageJ 1.31c (OS10.3) and NIH Image v1.63 (System 9.4); Wayne Rasband (NIH); Available at <http://rsb.info.nih.gov/ij/>•
Adobe Photoshop 8.0 (OS10.3); Adobe Systems, Inc.

Measurement of Area of Tissue Extractions for Contraction Analysis

1. Open ImageJ
2. Select File->Open and open desired file in .jpg, .bmp, or .tiff format
3. Select the *Straight-line selection tool*
4. Draw a line segment of known size (e.g. grid marks on graph paper).
5. Select Analyze->Set Scale
6. In the "Known distance" field, type in the known distance
7. In the "Unit of Length" field, type in the unit of the known distance
8. Select Process->Binary->Threshold
9. Use the *Eraser* to erase any points of contact between the Tissue Extractions and the background (grid lines of graph paper, etc)
10. Use the *Magic Wand* to select the perimeter of the Tissue Extractions
11. Select Analyze->Measure
12. Record measurement of area

Measurement of Lacuna and Inner Wound Area for Contraction Analysis

1. Repeat sets 1 through 7 above as above, in *Measurement of Area of Tissue Extractions for Contraction Analysis*
2. Use the *Magic Wand* to select the perimeter of interest
3. Select Analyze->Measure
4. Record measurement of area

Measurement of Scarring for Histological Analysis

1. Open ImageJ
2. Select File->Open to open an image of a glass hemacytometer.
3. Draw a line segment of known using the grids of the hemacytometer
4. Select Analyze->Set Scale
5. In the "Known distance" field, type in the known distance
6. In the "Unit of Length" field, type in the unit of the known distance
7. Record the resulting scale factor (pixels/unit distance)
8. Use the *Magic Wand* tool to trace the boundary between abnormal, scarred tissue and the surrounding normal renal parenchyma

9. Select Analyze->Measure
10. Record measurement of area

Measurement of Collagen Deposition

1. Open image using Adobe Photoshop.
2. Select Image->Adjustments->Replace Color
3. Click on the Dropper icon, and select a representative (blue) region of known collagen deposition
4. Set the Fuzziness to a level such that the preview window indicates that all regions of collagen deposition
5. If necessary, repeat steps 3 and 4 until the areas of collagen deposition are completely and exclusively selected.
6. Drag the Lightness slider so that the value reads -100
7. Click OK
8. Save the file in jpeg format
9. Open file using NIH Image
10. Select Analyze->Set Scale
11. In the "Units" field, type in the unit of the known scaling factor as per Step 7 the calibration in Measurement of Scarring for Histological Analysis
12. In the "Known distance" field, type in the value known scaling factor
13. Select Options-> Threshold.
14. Adjust the threshold to the appropriate level using the LUT slider window, such that only the pixels corresponding to collagen remain
15. Select Analyze->Measure
16. Record the measured area

APPENDIX E:
CONDITION OF TISSUE EXTRACTIONS

Wound Number	Mass (g)	Physical Condition	Wound Number	Mass (g)	Physical Condition
2a	0.0077	torn	12a	0.0114	cyl, sl. Torn
2b	0.0127	cyl	12b	0.0078	cyl, torn
2c	0.0142	cyl/cone	12c	0.0117	2 pieces
2d	0.0148	cone	12d	0.0092	cyl, torn
3a	0.0081	cyl, thin	13a	0.0093	2 pieces
3b	0.0119	cyl, angled	13b	0.0066	cone/cyl, torn
3c	0.0157	cyl, sl. Torn	13c	0.0115	cone, torn
3d	0.0067	torn	13d	0.01	cyl, torn
4a	0.0084	cyl, torn	14a	0.0096	chunk, oval
4b	None	None	14b	0.0147	cone/cyl
4c	0.0066	4 pieces	14c	0.0138	cyl
4d	0.0144	chunk	14d	0.0094	thin cyl
5a	0.0071	cyl	15a	0.0068	chunk
5b	0.01	cyl, torn	15b	0.0099	cone, irreg
5c	0.014	cyl/cone	15c	0.0094	cyl, torn
5d	0.0147	cone	15d	0.0098	cone, irreg
6a	0.0049	cyl, torn	16a	0.0078	chunk
6b	0.0069	cyl, angled	16b	0.0106	thin cyl
6c	0.0176	2 pieces	16c	0.0115	cone/cyl
6d	0.0052	cyl, torn	16d	0.0135	cyl
7a	0.0101	chunk	17a	0.0093	cyl/chunk
7b	0.0109	cyl/cone	17b	0.0109	thin cyl/torn
7c	0.0111	cyl, nice	17c	0.0078	flat cyl
7d	0.027	2 pieces	17d	0.0082	cone/torn
8a	0.0053	cyl, torn	18a	0.0095	thin cyl/torn
8b	0.0065	3 pieces	18b	0.0099	cone
8c	0.0113	cyl, nice	18c	0.011	cone
8d	0.0042	sm. Chunk	18d	0.0091	cone
9a	0.0054	cyl, flat	19a	0.0099	cyl
9b	0.008	chunk	19b	0.0122	cyl
9c	0.0081	flat, cyl	19c	0.0084	cyl/cone
9d	0.0061	3 pieces	19d	0.0117	cyl/cone
10a	0.0076	cyl, chunk	20a	0.0121	flat cyl
10b	0.0083	chunk	20b	-	missing
10c	0.0031	sm. Chunk	20c	0.0144	nice cone
10d	0.0052	chunk	20d	0.009	nice cone
11a	0.0097	cyl/cone			
11b	0.007	chunk			
11c	0.005	sm. Chunk			
11d	0.0051	chunk			

Table E.1: Mass and physical condition of excised tissue sample

REFERENCES

1. Townsend, Sabiston. 2001. *Textbook of Surgery*. 16th ed. Philadelphia: Saunders Company.
2. Geehan, Douglas. 2004. Renal Trauma. eMedicine. <<http://www.emedicine.com/med/topic2853.htm>>
3. Miller KS, McAninch JW. 1995. Radiographic assessment of renal trauma: Our 15 year experience. *J. Urol.* 154:352.
4. Seidman, Craig. 2003. Renal Trauma. Trauma.org. <<http://www.trauma.org/abdo/renal/management.html>>
5. Husmann DA, Gilling PJ, Perry MO, et al. 1993. Major renal lacerations with devitalized fragments following blunt abdominal trauma: A comparison between non-operative (expectant) versus surgical management. *J. Urol.* 150:1774-1777.
6. Radwin HM, Fitch WP, Robison JR. 1976. A unified concept of renal trauma. *J. Urol.* 116(1):20-2.
7. Armstrong, Paul, et. al. Management Strategies for Genitourinary Trauma. Wright State University School of Medicine. <<http://www.med.wright.edu/surg/divisions/trauma/gutrauma.htm>>
8. Ross R, Odland G. 1968. Human wound repair II: Inflammatory cells, epithelial-mesenchymal interactions, and fibrogenesis. *J. Cell Biol.* 39:152-168.
9. Yannas IV, Lee E, Orgill DP, Skrabut EM, Murphy GF. 1989. Synthesis and characterization of a model extracellular matrix that induces partial regeneration of adult mammalian skin. *Proc. Natl. Acad. Sci. USA* 86:933-7.
10. Goss RJ. 1992. Regeneration versus repair. *Wound Healing*, edited by Cohen IK, Diegelmann RF, and Lindblad WJ. Philadelphia: W.B. Saunders.
11. Cuppage FE, et al. 1967. Repair of the nephron following temporary occlusion of the renal pedicle. *Lab. Invest.* 17:660-674.
12. Madraza A, et al. 1970. Radiation nephritis II: Radiation changes after high doses of radiation. *Am. J. Pathol.* 61:37-56.

13. Oliver J. 1953. Correlations of structure and function and mechanisms of recovery in acute tubular necrosis. *Am. J. Med.* 15:535-557.
14. Vracko R, Benditt EP. 1972. Basal lamina: The scaffold for orderly cell replacement. *J. Cell Biol.* 55:406-419
15. Yannas IV. *Tissue and Organ Regeneration in Adults*. New York: Springer-Verlag 2001.
16. Hill B. 2004. *In Vivo Tissue Engineering in the Rat Kidney Using Collagen – Glycosaminoglycan Matrices*. Graduate Thesis. Cambridge: Massachusetts Institute of Technology.
17. Chamberlain LJ, Yannas IV, Hsu HP, Spector M. 2000. Connective tissue response to tubular implants for peripheral nerve regeneration: The role of myofibroblasts. *J. Comp. Neuro.* 417:415-430.
18. Hill, B. 2004. (Cited above)
19. Hill, B. 2004. Personal communication.

